

# Extraordinary properties of light transmission through a small chiral hole in a metallic screen

A V Krasavin, A S Schwanecke and N I Zheludev

EPSRC NanoPhotonics Portfolio Centre, School of Physics and Astronomy, University of Southampton, SO17 1BJ, UK

E-mail: [avk@soton.ac.uk](mailto:avk@soton.ac.uk)

Received 25 October 2005, accepted for publication 31 January 2006

Published 22 March 2006

Online at [stacks.iop.org/JOptA/8/S98](http://stacks.iop.org/JOptA/8/S98)

## Abstract

The true three-dimensional finite element numerical solution of Maxwell's equations shows that the propagation of light through a thin flat free-standing metallic screen containing a hole of twisted shape is sensitive to whether the incident wave is left or right circularly polarized. The intensity map and polarization state of light are dramatically changed depending on the mutual direction of the hole's twist and the incident light's wave polarization handedness. We also observed a strong concentration of the transmitted field at the centre of the chiral hole when light in the object plane rotates against the twist of the investigated gammadion type structure.

**Keywords:** planar chirality, metal nanostructures, extraordinary transmission, polarization

## 1. Introduction

The ability of left–right asymmetrical (chiral) three-dimensional (3D) molecules to rotate the polarization state of light, known as optical activity, is one of the most remarkable effects in optics that has been extensively studied since its discovery at the beginning of the 19th century. An optical active medium (e.g., a medium consisting of randomly oriented helix-like molecules) will show opposite signs of polarization azimuth rotation for the two mirror-symmetric (enantiomeric) forms of the constituting molecule. The general concept of chirality also exists in two dimensions, in which a planar object is said to be chiral if it cannot be brought into congruence with its mirror image unless it is lifted off the plane. One could therefore envisage a planar chiral medium that consists of 'flat' chiral elements possessing no line of symmetry in the plane.

Regular arrays of planar chiral elements have become the first type of object investigated for their optical properties [1]. It has been shown that light diffraction from a planar chiral array of gammadion-shaped micro-holes in a thin metal film is enantiomerically sensitive, i.e. the polarization state change of the diffracted light correlates with the sign of the gammadion twist, while their microscope images in polarized light display

unusual symmetries [2]. Recently, Prosvirnin and Zheludev conducted a theoretical analysis of the polarization eigenstates of partial waves diffracted on a planar chiral array that is consistent with the Lorentz theorem. They showed that eigenstates are bi-orthogonal for light diffraction in opposite directions and therefore are not necessarily the same [3]. Bi-orthogonality of the eigenstates leads to polarization eigenstate non-reciprocity in individual diffraction channels even when obeying the Lorentz reciprocity. This intriguing property has now been observed experimentally [4].

In this paper we study the propagation of light through a small *single* chiral hole in a metallic screen using numerical simulation. Metallic films structured on the nano-scale show a range of unusual properties, such as extraordinarily high transmission of light for perforation with round, rectangular and C-shaped holes [5–8], and strong linear birefringence for asymmetrical openings [9–11].

Here, we show that the propagation of light through a metallic screen containing a hole of twisted shape is sensitive to whether the incident wave is left (LCP) or right circularly polarized (RCP). The transmitted light accrues a component with handedness opposite to the incident wave, which peaks at a wavelength close to the hole's overall size. We also observed

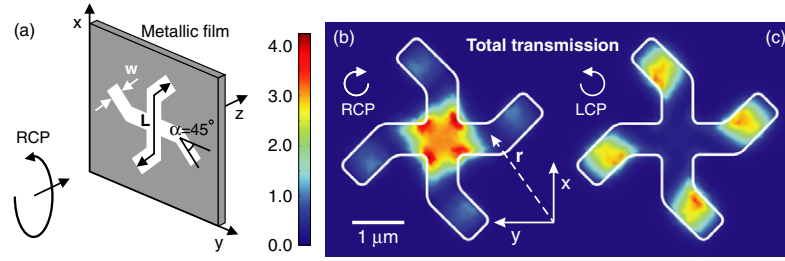


**Figure 1.** (a) Geometry and coordinate frame of the numerical experiment; (b) distribution of light intensity after passing a gammadion hole in an infinitely thin film of ideal metal at  $z = 140$  nm. A detailed physical description of the structure, the plotted intensity parameter  $s_0(\mathbf{r}, z)/s_{r,0}(0)$  and surrounding domains and normalization techniques can be found in section 3. Here and below the field maps are presented as seen from behind the hole and towards the light source.

a strong dependence of the distribution of light energy flow in the hole on the polarization state of incident radiation and note the concentration of the transmitted field at the centre of the chiral hole when the handedness of the chiral hole and the wave polarization state are the same.

## 2. Enantiomeric sensitive transmission

For our study of light transmission through a chiral hole, we examined gammadion-shaped openings of four-fold rotational symmetry in a plane metal screen. A gammadion is a star-like structure consisting of several rays or arms resembling the Greek capital letter  $\Gamma$ , which overall possesses a centre of rotation. The gammadion arms were bent at  $\alpha = 45^\circ$ , as shown in figure 1. This pattern is available in two mirror (enantiomeric) forms and is 2D chiral: it cannot be superimposed with its mirror image unless it is lifted from the plane. However, the structure, even when the hole is cut into the film of finite thickness, possesses no 3D chirality as its mirror image can be superimposed with the original by space rotations.

The gammadion handedness depends on whether the pattern is observed from one side of the screen or the other; in this paper, the gammadion handedness will be defined as seen by the *incident* light wave. We will distinguish clockwise and anti-clockwise twisted structures depending on the sign of their geometrical chirality index, as calculated according to the definition in [12] with positive chirality index indicating a clockwise structure. Then, as could be expected intuitively, gammadions with bending angle  $\alpha = +45^\circ$  are clockwise while gammadions with  $\alpha = -45^\circ$  are anti-clockwise. Thus, the gammadion in figure 1(a) is said to be clockwise. As we will be interested in the electromagnetic fields *transmitted* through the structure, the corresponding field maps will be presented as seen from the opposite side of the screen and looking into the incident light; see figures 1(b) and (c). All parameters of the incident and transmitted waves will be defined in the right-handed Cartesian coordinate frame shown in figure 1(a). Here the  $z$ -axis is directed perpendicular to the structure along the direction of the incident wave, while the axes  $x$  and  $y$  are directed along the cross-like central sections of the gammadion. The coordinate system origin is at the gammadion centre on the entrance plane on the screen, i.e. the plane  $z = 0$  coincides with the screen surface facing the incident wave.

For our numerical simulations we used the FEMLAB software package that implements a true 3D finite element method for solving Maxwell's equations in spectral representation [13] and was recently successfully used for electromagnetic calculations of complex plasmonics systems with large variation of scale parameters [14]. The simulations were performed on a 64-bit quadruple Opteron processor Linux-based workstation with 32 GB of RAM. The overall simulation domain had a cylindrical shape coaxial to the gammadion structure with  $8.4 \mu\text{m}$  diameter and  $3 \mu\text{m}$  height. All domain boundaries were chosen to be low-reflecting, while the cylindrical base surface was set as source of the wave incident on the structure. We used an iterative solver capable of dealing with large simulation problems with typically 4 million mesh elements. Average simulation time for a given wavelength when converging to 5% accuracy was about 4 h with visualization of individual field maps typically lasting another 20 min. The inevitable presence of domain boundaries affects the results. Nevertheless, our domain is sufficiently large so that further increase of the domain volume does not affect essential features and symmetries of the observed effects. Therefore, we may consider our simulational situation to be close to that of an infinite screen with a hole in a free-space environment.

The main result of our analysis is that transmission of light through the chiral gammadion opening is enantiomerically sensitive, i.e., the field distribution after the hole is sensitive to the mutual handedness of the field and the gammadion hole. In other words, it matters to the circularly polarized wave whether it passes through a clockwise or anti-clockwise gammadion hole. Enantiomeric sensitivity may be illustrated for the simplest situation of transmission through a chiral hole in an infinitely thin film of 'ideal' metal. Here, an ideal metal film is defined as imposing the boundary condition  $\mathbf{n} \times \mathbf{E} = \mathbf{0}$  on the fields of the wave, where  $\mathbf{n}$  is a unit vector normal to the surface. This condition sets the tangential component of the electric field on the surface to zero. On figure 1 we present a normalized distribution of the Stokes parameter  $s_0$  in the plane of the hole for the case when the wavelength of the incident light  $\lambda$  is in proximity to the gammadion size  $L$ . One can see that, when the handedness of the incident wave and the gammadion (as perceived from the wave source, see definition above) coincide, the electromagnetic field is concentrated in the centre of the structure (figure 1(a)), while for opposite handedness of incident wave and hole the field is concentrated in the gammadion branches (figure 1(b)). As the characteristic

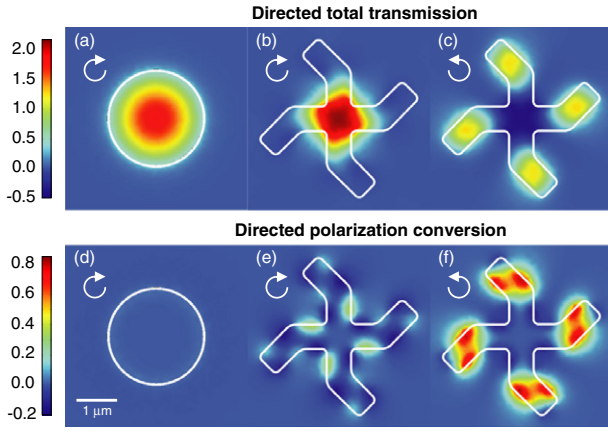


**Figure 2.** Transmission and polarization conversion for a round achiral hole and chiral gammadion hole at  $\lambda = 3 \mu\text{m}$ . Top row intensity maps are represented by  $P_z(\mathbf{r}, z)/P_z(\mathbf{r}, 0)$  for (a) a round hole with RCP incident light and for a gammadion hole with (b) RCP and (c) LCP incident waves. Bottom row polarization conversion maps are presented in terms of  $P_z^-(\mathbf{r}, z)/P_z^-(\mathbf{r}, 0)$  for (d) a round hole with RCP incident polarization and (e) a gammadion hole with RCP incident light, while with (f) LCP incident light the parameter  $P_z^+(\mathbf{r}, z)/P_z^+(\mathbf{r}, 0)$  is used. In all cases field maps are taken at  $z = 300 \text{ nm}$ . The arrows illustrate the polarization state of the incident wave.

dimensions of the hole are the only parameters with length dimension, one can expect geometrically resonant features of the effect to appear at wavelengths that are somehow related to the physical size of the gammadion.

Enantiomerically sensitive transmission is the effect which was discovered in 2005 [15]. Here, we report results of a much more detailed study of this phenomenon. In particular, since our first publication we have been able to substantially improve the accuracy of our calculations. We now provide much more detailed characteristics of the enantiomeric effect in particular towards the efficiency of polarization conversion and total transmission through the chiral hole. This, for the first time, includes a comparison of the total transmission and polarization conversion efficiencies on the basis of both Stokes and Poynting vector calculations. And finally, for the first time, we give full polarization maps of the transmitted light through a chiral hole which allow the observation of new polarization phenomena.

### 3. Chiral hole in gold film

From now on we will concentrate on a realistic case of transmission of a normally incident plane wave through a free-standing flat gold film of thickness  $d = 140 \text{ nm}$  with a single gammadion-shaped slit cut into it. The width of the gammadion slit  $w$  was chosen to be  $0.6 \mu\text{m}$ , while the total length of the gammadion, measured between ends of opposite arms, was  $L = 4.1 \mu\text{m}$ ; see figure 1(a). We used values of the complex dielectric coefficient of gold at different wavelengths from [16]. As for the case of a chiral hole in an infinitely thin film of ideal metal, the field distributions are enantiomerically sensitive. Figure 2 illustrates this for  $\lambda = 3 \mu\text{m}$ , where maps of  $P_z(\mathbf{r}, z)/P_z(\mathbf{r}, 0)$  are presented for RCP (figure 2(b)) and LCP incident light (figure 2(c)), respectively, and with  $P_z(\mathbf{r}, 0)$

referring solely to the incident wave discarding any resulted reflections from the screen. These maps are taken at  $160 \text{ nm}$  from the screen, i.e. at  $z = 300 \text{ nm}$ .

From comparison of the intensity distributions one can easily see that transmission through the chiral gammadion hole is enantiomerically sensitive: there is a dramatic difference depending on the mutual direction of the hole's twist and the polarization handedness of the incident wave; see figure 2. When the handednesses of the gammadion hole and of the incident light wave are the same, light is concentrated in the central region of the gammadion, while in the opposite case it is concentrated in the outer regions of the gammadion. We compare intensity distributions of light transmitted through the gammadion opening with that of light transmitted through a round hole; see figure 2. The dimension of the round hole was chosen to occupy the same area as the gammadion opening. We observed that, as can be expected, the transmission intensity maps do not depend on whether the incident light is right or left circularly polarized (presented here are only maps for RCP illumination).

Propagation of light through the small hole, comparable with the wavelength, is accompanied by diffraction and leads to the appearance of strong non-paraxial components in the transmitted field. In this study we will only be interested in the energy flow in the direction along the screen normal at various distances from the screen. Similarly, we will investigate the polarization characteristics of this component of transmitted radiation as defined by the Stokes parameters:

$$\begin{aligned} s_0 &= E_x E_x^* + E_y E_y^*, \\ s_1 &= E_x E_x^* - E_y E_y^*, \\ s_2 &= 2 \text{Re}\{E_x^* E_y\}, \\ s_3 &= 2 \text{Im}\{E_x^* E_y\}. \end{aligned} \quad (1)$$

The first component of the Stokes parameter  $s_0$  presented here is a widely used measure, which for a plane wave shows the distribution of the energy flow. However, in the proximity of a border, approximating the energy flow in a highly divergent wave, such as one emerging from a small chiral hole, by  $s_0$  may give results different from using the  $z$ -projection of the Poynting vector  $P_z$ . However, these small differences between  $s_0$  and  $P_z$  distributions can be observed for both the field maps and the transmission integral parameters.

We introduce the integral transmission parameters  $S$  and  $T$  as

$$S(z) = \int s_0(\mathbf{r}, z) d^2\mathbf{r} / \int_{\Gamma} s_0(\mathbf{r}, 0) d^2\mathbf{r} \quad (2)$$

and

$$T(z) = \int P_z(\mathbf{r}, z) d^2\mathbf{r} / \int_{\Gamma} P_z(\mathbf{r}, 0) d^2\mathbf{r} \quad (3)$$

with  $d^2\mathbf{r} = dx dy$  and the normalizations  $s_0(\mathbf{r}, 0)$  and  $P_z(\mathbf{r}, 0)$  referring solely to the incident wave ignoring any resulted reflections; furthermore, as above,

$$P_z = \frac{1}{2} \text{Re}\{E_x H_y^* - E_y H_x^*\}. \quad (4)$$

For the purpose of normalization, the integrals at  $z = 0$  are taken over the area of the gammadion opening  $\Gamma$ , while behind the screen integration is taken over the whole  $xy$ -plane.

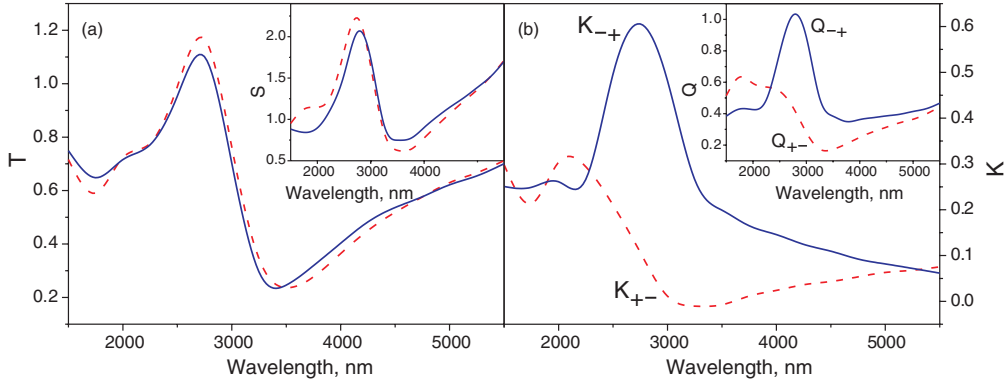


**Figure 3.** Shown are the spectral dependences for a chiral gammadion hole: integral transmission ( $S$ ,  $T$ ) and polarization conversion ( $Q$ ,  $K$ ) for circularly polarized light in terms of the Stokes parameter ( $S$ ,  $Q$ ) and Poynting vector ( $T$ ,  $K$ ) representations. Solid lines correspond to LCP illumination, dashed to RCP.

(This figure is in colour only in the electronic version)

We also found that the transmitted light accrues a polarization component opposite to the polarization state of the incident wave, giving rise to a circular polarization conversion effect. Thus, the transmitted field becomes elliptically polarized. To describe this effect we introduce the following integral parameters for conversion of a RCP state into a LCP state.

$$Q_{+-} = \int \frac{s_0(\mathbf{r}, z) + s_3(\mathbf{r}, z)}{2} d\sigma \bigg/ \int_{\Gamma} s_0(\mathbf{r}, 0) d\sigma \quad (5)$$

and

$$K_{+-} = \int P_z^-(\mathbf{r}, z) d\sigma \bigg/ \int_{\Gamma} P_z(\mathbf{r}, 0) d\sigma. \quad (6)$$

Correspondingly, for the conversion of a LCP wave into the RCP state we define

$$Q_{-+} = \int \frac{s_0(\mathbf{r}, z) - s_3(\mathbf{r}, z)}{2} d\sigma \bigg/ \int_{\Gamma} s_0(\mathbf{r}, 0) d\sigma \quad (7)$$

and

$$K_{-+} = \int P_z^+(\mathbf{r}, z) d\sigma \bigg/ \int_{\Gamma} P_z(\mathbf{r}, 0) d\sigma. \quad (8)$$

Here,  $\frac{1}{2}(s_0(\mathbf{r}, z) \pm s_3(\mathbf{r}, z))$  represent the intensity of the circularly polarized component of the transmitted wave for LCP and RCP respectively in terms of the Stokes parameters  $s_0$  and  $s_3 = 2 \text{Im}\{E_x^* E_y\}$ , while

$$P_z^- = \frac{1}{4} \text{Re}\{-iE_x H_x^* + E_x H_y^* - E_y H_x^* - iE_y H_y^*\} \quad (9)$$

and

$$P_z^+ = \frac{1}{4} \text{Re}\{iE_x H_x^* + E_x H_y^* - E_y H_x^* + iE_y H_y^*\} \quad (10)$$

are Poynting vector projections on the  $z$ -direction for the LCP and RCP components of the field.

Both integral transmission parameters,  $S$  and  $T$ , show pronounced wavelength dependences for the transmission of circularly polarized light through a clockwise gammadion hole with a peak at a wavelength of 2750 nm; see figure 3. In terms of parameter  $S$  we observed differential transmission for RCP and LCP light. However, the total observable transmission as measured by parameter  $T$  is within the computational accuracy

the same for RCP and LCP incident light; see figure 3(a). This seems to make the possibility of circular differential transmission through a chiral hole difficult.

However, differential polarization conversion for RCP and LCP incident polarizations is an effect which is clearly seen in terms of both parameters  $S$  and  $T$ ; see figure 3(b). For a clockwise hole in resonance, conversion of LCP polarization into RCP is much more efficient than conversion of RCP into LCP. (Correspondingly, for an anti-clockwise hole conversion of RCP into LCP will be more efficient than conversion of LCP into RCP.) Field maps illustrating this dramatic difference for polarization conversion at the maximum of the differential conversion effect are presented in figure 2. We compare polarization conversion with that for light transmitted through an achiral round hole, see figure 2(d), where this effect naturally is not to be found.

Here, we would like to note that the observed polarization conversion effect with circularly polarized light is governed by the chirality of the hole. It is different in its manifestation and nature from the well documented polarization conversion effect for linearly polarized light, which is driven by anisotropy of the structure and may be seen in a metal grating consisting of a series of high and narrow ridges oriented at  $45^\circ$  to the polarization angle [17].

We found that all transmission characteristics for RCP light through a clockwise hole are exactly the same as for an LCP wave through an anti-clockwise hole, while integral transmission of RCP light through an anti-clockwise hole is identical to that of an LCP wave through a clockwise hole. We therefore present only results for transmission through one type, a clockwise gammadion hole.

From here, one can make the intriguing observation that since the perceived sense of twist of the chiral hole depends on what side the screen is observed from, the field properties and in particular the polarization conversion efficiency depend on whether the light wave enters the screen from one side or the other.

#### 4. Nano-focusing

When the handednesses of the gammadion and incident polarization state coincide, the light field behind the screen

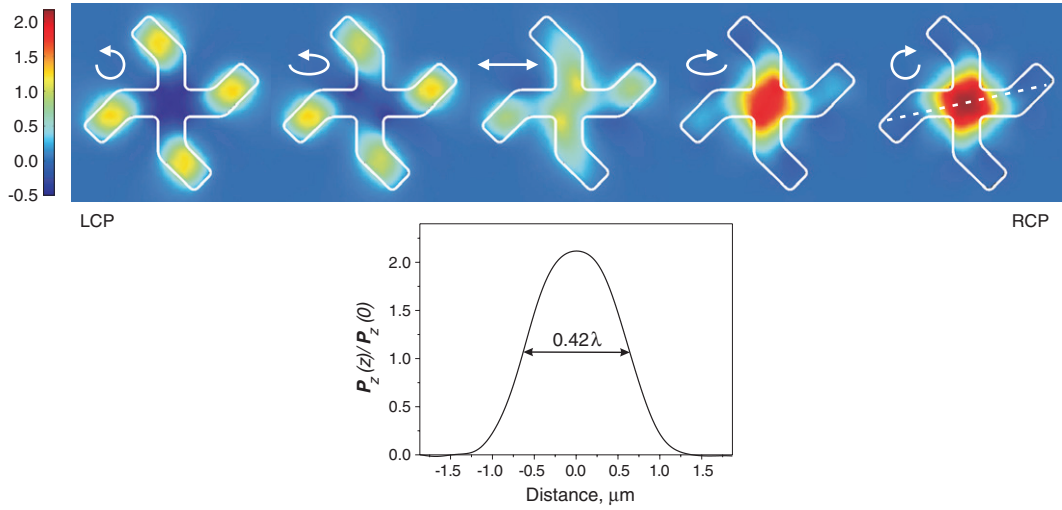


**Figure 4.** The transmitted intensity  $P_z(\mathbf{r}, z)/P_z(\mathbf{r}, 0)$  behind the gammadion hole depends on the polarization state of the incident light, as indicated by adjacent arrows. Below is an intensity profile plot, which was taken along the direction indicated by the dashed line on the field map to the far right for RCP illumination.

is concentrated at the gammadion centre in a spot which is smaller than both the wavelength and the characteristic size of the gammadion. In contrast, when the handednesses of the gammadion and incident wave are opposite, light energy is spread over the opening. This gives an opportunity for polarization-controlled nano-focusing, illustrated in figure 4: continuous change of the incident polarization state from LCP to RCP does not affect the total power of light passing through the hole while, however, changing its concentration in the gammadion centre. Note that intensity concentration in the case of RCP illumination is higher and more strongly localized than in the case of transmission through a round hole; see figure 2.

## 5. Polarization state of light transmitted through a chiral hole

As a chiral opening dramatically changes the polarization state of light, we investigated this interesting aspect more thoroughly. In all our calculations we controlled the degree of polarization of transmitted light

$$\rho(\mathbf{r}, z) = \frac{\sqrt{s_1^2(\mathbf{r}, z) + s_2^2(\mathbf{r}, z) + s_3^2(\mathbf{r}, z)}}{s_0(\mathbf{r}, z)} \quad (11)$$

where  $\mathbf{r} = (x, y)$ .

By definition  $\rho = 1$  for a totally polarized wave. We found that  $\rho(\mathbf{r}, z) = 1$  for light transmitted through a chiral gammadion hole. The polarization state of the totally polarized light may be described by its degree of ellipticity  $\eta$  and its polarization azimuth  $\theta$ . These parameters are defined from the Stokes parameters of the wave as follows:

$$\tan 2\theta(\mathbf{r}, z) = \frac{s_2(\mathbf{r}, z)}{s_1(\mathbf{r}, z)} \quad (12)$$

and

$$\eta(\mathbf{r}, z) = \frac{s_3(\mathbf{r}, z)}{s_0(\mathbf{r}, z)}. \quad (13)$$

Figures 5 and 6 show maps of the degree of ellipticity  $\eta(\mathbf{r}, z)$  and polarization azimuth  $\theta(\mathbf{r}, z)$  at various distances  $z$  from the screen and for different incident circular polarizations. To show the space evolution of the polarization state we plotted  $\eta$  and  $\theta$  starting at 160 nm from the screen, i.e. at  $z = 300$  nm, just behind the gammadion opening, and finishing at approximately half the wavelength distance  $z = 1580$  nm, in steps of 320 nm.

Colour-coded field maps for ellipticity are presented in figure 5. There, small black arrows indicate the polarization azimuth, i.e. orientation of the main axis of the polarization ellipse. The length of the black arrows correlates with the light intensity.

At a short distance from the screen in the case of RCP illumination the light is concentrated at the centre of the structure, where light remains circularly polarized and the handedness of the polarization state of the incident light is preserved (red spot in the centre). For the case of LCP illumination the energy flow is concentrated in the regions of the outer gammadion sections, where the polarization state to a good approximation is linear (green areas). Here, the energy flow through the central region is weak.

At larger distance from the screen, see for example  $z = 1580$  nm, in the case of RCP illumination (left sequence in figure 5) the light intensity remains concentrated near the main axis of the system where the polarization state remains circular (see the central red region on the maps).

In the case of LCP illumination (right sequence in figure 5) the beam divergence is much stronger. At a distance of 1580 nm the original polarization state on the main axis is preserved. However, in the outer regions, where energy is concentrated, one can observe almost total conversion to the opposite, RCP state (intense red regions).

Maps for the polarization azimuth are presented in figure 6. At a distance of 160 nm from the screen,  $z = 300$  nm, and for RCP illumination the polarization azimuth lines create a saddle structure with its centre at the  $z$ -axis. At larger distances (see for example  $z = 1580$  nm) the saddle structure

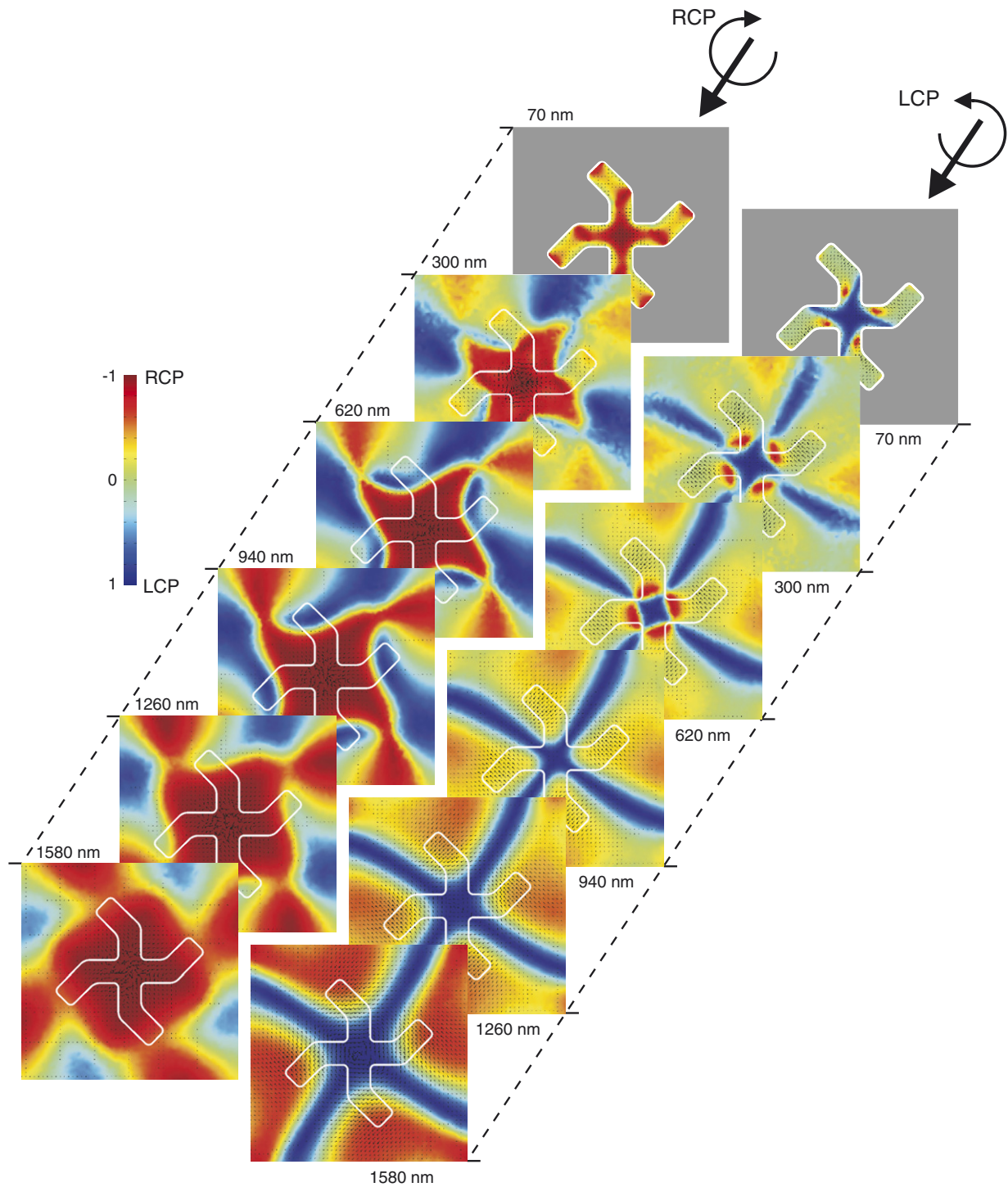


**Figure 5.** Colour maps illustrate the ellipticity  $\eta$  of light transmitted through a chiral hole at different distances from the screen for RCP (left series) and LCP (right series) incident light.

disappears as the polarization state in the centre becomes close to RCP.

For LCP illumination at a distance of  $z = 300$  nm the polarization state in the outer gammadion regions is linear and oriented across its branches, i.e. perpendicular to the metallic walls of the structure. This may be connected to surface plasmon polariton excitation aided transmission, which favours this particular polarization azimuth.

## 6. Discussion

The revealed phenomena open an extensive arena for future investigation. We expect for instance a direct connection between the magnitude of the observed effects and the angle at which the gammadion arms are bent, as this is directly connected with the geometrical asymmetry or planar chirality

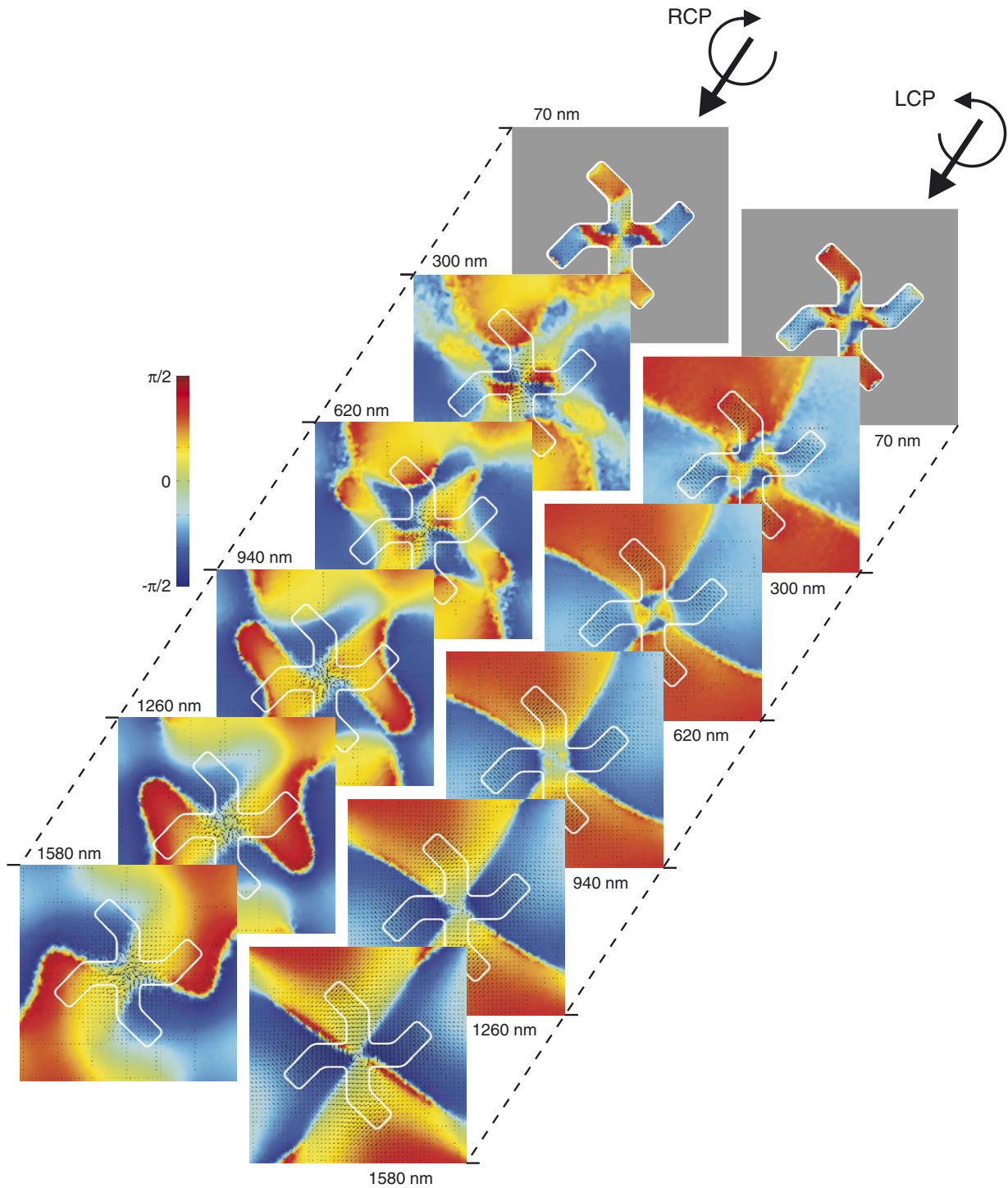


**Figure 6.** Colour maps illustrate the polarization azimuth  $\theta$  of light transmitted through a chiral hole at different distances from the screen for RCP (left series) and LCP (right series) incident light.

of the gammadion. In these terms, the optical activity should vanish for a bending angle of  $0^\circ$ , corresponding to the case of an achiral cross. On the other hand, the magnitude of the effect might decrease and even change sign if the angle gets bigger than  $90^\circ$ , in accordance with predictions and calculations following the geometrical analysis of [12]. This likewise encourages future simulations regarding the connection of

measures of chirality and electromagnetic properties of planar chiral structures in general.

Equally important is a thorough investigation of the dependence of the light transmission on the thickness of the film in which the chiral structure is embedded. This would also reveal the possible role of surface plasmon polariton excitations on the inner walls of the gammadion hole and offer

guidance towards an exploitation of the combined properties. Apart from that, a move of the simulation frequencies towards the optical region will approach the plasma frequency of the metal and possibly add new effects or enhancements of the already known ones.

Topological features of the polarization maps created by transmission through a chiral hole are a very interesting yet not explored field deserving attention. The recent discovery of whirlpool-like optical vortices in the energy flow lines near metal nanoparticles at plasmon resonance [18] calls for the search of similar singularities of chiral symmetry in planar structures. An intriguing challenge is, furthermore, to understand the coupling of orbital and spin moments of light beams interacting with planar chiral structures and to evaluate the angular momentum transfer between the structure and the light beam [19].

Another interesting direction is the introduction of dielectric material on one side (or possibly both) of the metal film. This will violate the symmetry along the  $z$ -axis and may result in new phenomena in systems now being as well truly 3D chiral apart from their original 2D chirality, discussed for example by Bedeaux *et al* [20] and corresponding to substrate-based samples used in [1] and [2]. Our initial simulations revealed that in this case not only will the field distribution and polarization properties depend on the handedness of the illuminating light, but the total energy of the transmitted light as well. Moreover, recent research showed that the introduction of absorption in such layers may be the source of a completely different response of planar structured layers [21]. Naturally, an investigation of a widened range of chiral topologies should be performed, including structures of different rotational symmetry.

Analytical theory explaining the broken enantiomeric symmetry of light transmission through a chiral hole and its analytical description in term of non-paraxial non-local optics is now being developed [22].

Overall, the combined spectral and polarization properties of chiral nano-holes and, in particular, for those of four-fold rotational symmetry, will allow their implementation in a number of existing devices as well as novel ones. On the one hand, they could be part of standard optical components for free-space applications like polarizers or phase retarders and wave-plates with tunable spectral capabilities and novel components for manipulating the polarization state of light in the near-field in nano-photonics devices. On the other hand, their use in novel non-reciprocal devices or the exploitation of polarization-controlled 'nano-lensing' might open completely new doors. The latter would for example allow for far-field controlled near-field concentrations with broad applications for nano-lithography and bio-imaging. The advantage of this planar type of structures, in any case, will be that its necessary thickness is only a fraction of the wavelength, in contrast with bulky conventional systems based on light propagation in crystalline media or diffraction-based systems.

## 7. Conclusions

We numerically investigated the polarization state and integral characteristics of enantiomerically sensitive transmission and polarization conversion of circularly polarized light through a chiral hole in a metallic screen, as well as a corresponding nano-focusing effect.

## Acknowledgments

The authors acknowledge the support of the Engineering and Physical Sciences Research Council (UK) and the EU Network of Excellence Metamorphose, as well as fruitful discussions with Anatoly Zayats, Mark Dennis, Matthias Reichelt, Tineke Stroucken, Stephan Koch, and Ewan Wright.

## References

- [1] Papakostas A, Potts A, Bagnall D M, Prosvirnin S L, Coles H J and Zheludev N I 2003 *Phys. Rev. Lett.* **90** 107404
- [2] Schwanecke A S, Krasavin A, Bagnall D M, Potts A, Zayats A V and Zheludev N I 2003 *Phys. Rev. Lett.* **91** 247404
- [3] Prosvirnin S L and Zheludev N I 2005 *Phys. Rev. E* **71** 037603
- [4] Potts A, Papakostas A, Bagnall D M and Zheludev N I to be published
- [5] Ebbesen T W, Lezec H J, Ghaemi H F, Thio T and Wolff P A 1998 *Nature* **391** 667
- [6] Garcia de Abajo F G 2002 *Opt. Express* **10** 1475
- [7] van der Molen K L, Koerkamp K J, Enoch S, Segerink F B, van Hulst N F and Kuipers L 2005 *Phys. Rev. B* **72** 045421
- [8] Matteo J A, Fromm D P, Yuen Y, Schunk P J, Moerner W E and Hesselink L 2004 *Appl. Phys. Lett.* **85** 648
- [9] Elliott J, Smolyaninov I I, Zheludev N I and Zayats A V 2004 *Opt. Lett.* **29** 1414
- [10] Gordon R, Brolo A G, McKinnon A, Rajora A, Leathem B and Kavanagh K L 2004 *Phys. Rev. Lett.* **92** 037401
- [11] Degiron A, Lezec H J, Yamamoto N and Ebbesen T W 2004 *Opt. Commun.* **239** 61
- [12] Potts A, Bagnall D M and Zheludev N I 2004 *J. Opt. A: Pure Appl. Opt.* **6** 193
- [13] Jin J 2002 *The Finite Element Method in Electrodynamics* (New York: Wiley)
- [14] Krasavin A V and Zheludev N I 2004 *Appl. Phys. Lett.* **84** 1416–8
- [15] Krasavin A V, Schwanecke A S, Zheludev N I, Reichelt M, Stroucken T, Koch S W and Wright E M 2005 *Appl. Phys. Lett.* **86** (20)
- [16] Palik E D (ed) 1984 *Handbook of Optical Constants of Solids* (New York: Academic)
- [17] Hooper I R and Sambles J R 2002 *Opt. Lett.* **27** 2152
- [18] Bashevov M V, Fedotov V A and Zheludev N I 2005 *Opt. Express* **13** 8372
- [19] Wright E M and Zheludev N I 2003 *Preprint cond-mat/0310023*
- [20] Bedeaux D, Osipov M A and Vlieger J 2004 *J. Opt. Soc. Am. A* **20** 2431–41
- [21] Fedotov V A, Mladyonov P L, Prosvirnin S L and Zheludev N I 2005 *Phys. Rev. E* **72** 056613 (Fedotov V A, Mladyonov P L, Prosvirnin S L and Zheludev N I 2005 *Preprint cond-mat/0504761*)
- [22] Reichelt M, Stroucken T, Koch S W, Krasavin A V, Schwanecke A S, Zheludev N I, Moloney J V and Wright E M to be published